Pentiptycene Polymer/Single-Walled Carbon Nanotube Complexes: Applications in Benzene, Toluene and o-Xylene Detection

Journal:	*ACS Nano*
Manuscript ID	nn-2020-02570y.R3
Manuscript Type:	Article
Date Submitted by the Author:	n/a
Complete List of Authors:	Luo, Shao-Xiong Lennon; Massachusetts Institute of Technology Department of Chemistry, Lin, Che-Jen; National Dong Hwa University, Chemistry Ku, Kang Hee; Massachusetts Institute of Technology, Chemistry Yoshinaga, Kosuke; MIT, Swager, Timothy; Massachusetts Institute of Technology, Chemistry

Pentiptycene Polymer/Single-Walled Carbon Nanotube Complexes: Applications in Benzene, Toluene and *o*-Xylene Detection

Shao-Xiong Lennon Luo[†], Che-Jen Lin[†§], Kang Hee Ku, Kosuke Yoshinaga and Timothy M. Swager*

Department of Chemistry and Institute for Soldier Nanotechnologies, Massachusetts Institute of Technology, 77 Massachusetts Avenue, Cambridge Massachusetts 02139, United States

ABSTRACT: We report the dispersion of single-walled carbon nanotubes (SWCNTs) using pentiptycene polymers and their use in chemiresistance-based and QCM-D sensors. Poly(*p*-phenylene ethynylene)s (PPEs) incorporating pentiptycene moieties present a concave surface that promotes π–π interactions and van der Waals interactions with SWCNT. In contrast to more common polymer-dispersing mechanisms that involve the wrapping of polymers around the SWCNTs, we conclude that the H-shape of pentiptycene groups and the linear rigid-rod structure creates a slot for nanotube binding. UV-Vis-NIR, Raman, fluorescence spectra and TEM images of polymer/SWCNTs support this dispersion model which shows size selectivity to SWCNTs with diameters of 0.8−0.9 nm. Steric bulk on the channels is problematic and *tert*-butylated pentiptycenes do not form stable dispersions with SWCNTs. This result, along with the diameter preference supports that model that the SWCNTs are bound to the concave clefts of the pentiptycenes. The binding model suggests that the polymer/SWCNTs complex create galleries and we have demonstrated the binding of benzene, toluene and *o*-xylene (BTX) vapors as the basis for a robust, sensitive and selective sensing platform for BTX detection. The utility of our sensors is demonstrated by the detection of benzene at the OSHA short-term exposure limit of 5 ppm in air.

KEYWORDS: carbon nanotubes, pentiptycene polymer, polymer/carbon nanotube composites, benzene sensing, chemiresistive sensing, quartz crystal microbalance with dissipation monitoring

Single-walled carbon nanotubes (SWCNTs) are attractive materials for sensing gaseous analytes as a result of their sensitive resistance changes in response to the binding of molecules.[1–5] The sensing performance in these materials is a consequence of a high surface area-to-volume ratio, molecular adsorption onto their electronically active sidewalls, swelling of the matrix, and/or their restricted conduction pathways.[5] However, pristine SWCNTs display non-specific responses to chemical exposures and covalent or noncovalent functionalization with selectors or receptors is required to produce selectivity to target analytes. Covalent functionalization utilizes reactions that attach chemical groups covalently to the conjugated surfaces or termini of CNTs.[6–9] Covalent functionalization has the advantage that it produces stable anchors of functional groups to CNT. However, covalent attachment of groups to the graphene surface transforms sp^2 carbons into sites with increased sp^3 character that disrupts electronic coherence and decreases carrier mobility. Noncovalent functionalization of SWCNTs is less perturbative to the electronic properties of the nanotubes and the associated higher carrier mobilities can provide enhanced sensitivity.[10–15]

As chemiresistive sensors, SWCNTs have been functionalized noncovalently by physisorption of small aromatic molecules and surfactants through π–π and hydrophobic interactions.[16–25] Physisorbed selector molecules or coatings often have limited stability and are prone to environmentally induced changes in their configuration around the CNT, can undergo phase segregation, and can desorb in solution leading to unstable dispersions. These changes can produce large conductance changes that give rise to drift and degraded performance in chemiresistive sensors. Polymer wrapping or surface anchored molecular clips produces stable noncovalent functionalized SWCNTs[26–34] and has also been widely explored to separate and purify[35–47] or orient[48,49] these materials. Conjugated polymers with selectors attached can provide selectivity for the detection of specific analytes and even resolve structural isomers of xylenes.[13, 50–53] Simple poly(phenylene ethynylene)s (PPEs) have been shown to disperse SWCNTs[54–58] and we have been interested to see if PPEs containing pentiptycene, a rigid H-shaped molecule with a cleft of about 10 Å diameter (**Figure 1a**),[59] would have strong interactions with SWCNTs of a complementary diameter. Pentiptycene's structural properties in conjugated oligomers[60,61] and polymers[62,63] prevent intermolecular π–π interactions to maintain high photoluminescence in solid films. The free volume in these structures creates porous structures that have provided size exclusion for the selective detection of small molecule analytes.[64–67]

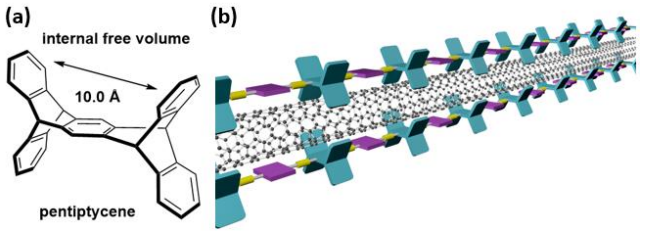

Figure 1. (a) Structural property of pentiptycene (b) schematic drawing of dispersion mechanism of SWCNT between pentiptycene polymers.

In this report we propose the dispersion method illustrated in a simplified form in **Figure 1b**, wherein rather than wrapping around a SWCNT, pentiptycene functions as a linear arrangement of clips that cooperatively bind through Van der Waals interactions. Central to this model is that the diameter of the cleft defined by the pentiptycene matches SWCNT with a diameter of about 0.9 nm. Commercially-available SWCNTs have a size distribution and we expect pentiptycene polymers to selectively disperse SWCNTs of a complementary size. To this end we designed five pentiptycene-incorporating polymers, **P1**–**P5** (**Chart 1**), and investigated their dispersions with SWCNTs. All of the polymers contain long alkyl chains to enhance solubility. **P3** and **P5** also contain bulky *tert*-butyl groups on the periphery ring of pentiptycene that has been shown to increase free volume in polymers.[68] The polymer/SWCNT dispersions and thin films were characterized by UV-Vis-NIR absorption, photoluminescence, Raman scattering, and TEM imaging. We further demonstrate that the polymer/SWCNT constructions impart enhanced selective sensing responses to vapors of benzene, toluene, and *o*-xylene (BTX).

Chart 1. Chemical structures of **P1**–**P5**

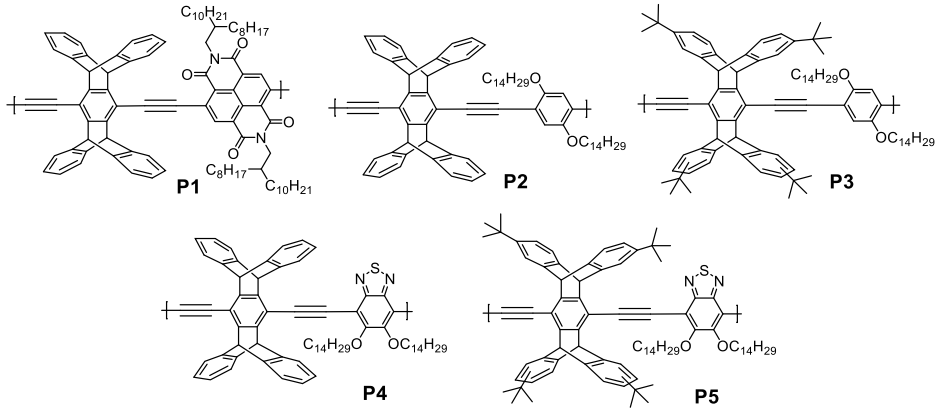

RESULTS AND DISCUSSION

The polymer/SWCNT dispersions were prepared according to the following procedure. The pentiptycene polymer (3 mg) was dissolved in chlorobenzene (4 mL) with 2 mg of CoMoCAT SWCNTs CG100. After 30 min of tip sonication at 63 Watts, the suspension was centrifuged for 4 hours at 30130 g. The CG100 SWCNT dispersions with **P1**, **P2** and **P4** have high stability and are optically opaque after centrifugation. In contrast, dispersions using *tert*-butylated pentiptycene polymers, **P3** and **P5**, are unstable and yield clear solutions after centrifugation. The optical absorbance of the supernates obtained directly after the centrifugation was analyzed in a 1 mm short-path quartz cuvette (**Figure 2**). For **P1**/CG100, **P2**/CG100 and **P4**/CG100, clear interband transitions of the van Hove singularities were observed in the absorption features. Absorption peaks in S_{11} (830–1600 nm) and S_{22} (600–800 nm) regions indicate the presence of semiconducting SWCNTs whereas the broad and featureless absorption background and peaks in M_{11} (440–645 nm) region indicate the presence of metallic SWCNTs.[69] (6,5), (7,6), (7,5) and (8,7) SWCNTs were found to be the major species in the polymer/SWCNT dispersions.[70–72] Notably, **P4**/CG100 has much sharper absorption peaks than **P1**/CG100 and **P2**/CG100, suggesting the superior polymer/SWCNT dispersion quality by **P4**. The absorption features of **P1**/CG100 in the S_{11} (830–1600 nm) region are slightly broader than those of **P2**/CG100 and **P4**/CG100, which suggests mild bundling of SWCNTs possibly due to the branched alkyl chains in **P1** which could hinder the polymer/SWCNT interaction.[44] On the contrary, no clear absorption feature was identified for **P3**/CG100 and **P5**/CG100 as they failed to yield stable SWCNT dispersions. The fact that the bulky *tert*-butylated pentiptycene polymers display poor SWCNT dispersion is also consistent with the binding to the SWCNT being mediated by strong Van der Waals interactions between the π-systems.

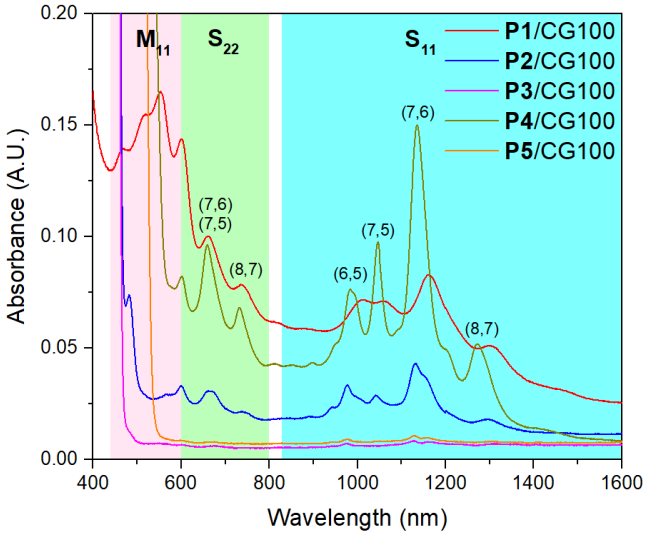

Figure 2. UV−vis−NIR absorption spectra of supernates of **P1**/CG100 (red), **P2**/CG100 (blue), **P3**/CG100 (purple), **P4**/CG100 (green) and **P5**/CG100 (orange). The pink, green and cyan boxes indicate the locations of optical transitions of metallic (M_{11}) and semiconducting (S_{22}, S_{11}) SWCNTs, respectively. Characteristic absorption peaks are labeled with the assigned chirality.

To support our proposed non-covalent structural model, we collected Raman spectra of the polymer/SWCNT complexes (**Figure S3**). Thin film samples were prepared by drop-casting polymer/CG100 supernatant dispersions onto silicon wafers. A pristine CG100 SWCNT thin film was also

prepared for reference. The spectra were obtained using 633 nm excitation wavelength and are normalized to the intensity of the G-band, at 1590 cm^{-1}. The D-band, located at around 1300 cm^{-1}, is indicative of the disruption of the sp^2 network in conjugated nanocarbon systems and the intensity ratio of the D to G bands (I_D/I_G) provides information of the perturbation of the π-system. The I_D/I_G of polymer/CG100 films were 0.05–0.07, which is close to that of pristine CG100 (0.05) and confirms minimal disruption of the nanotubes electronic structure.

The need to match the SWCNT diameter with the size of the pentiptycene cleft was evaluated in dispersions using **P4** and several commercial SWCNTs with different diameter distributions. Beside CoMoCAT SWCNTs CG100 (0.7–1.3 nm diameter), HiPCO SWCNTs (0.8–1.2 nm diameter), (6,5)-enriched CoMoCAT SWCNTs SG65i (0.7–0.9 nm diameter) and arc-discharge SWCNTs CarboLex (1.2–1.5 nm diameter) were investigated. The UV-Vis-NIR spectra of the dispersions are shown in **Figure 3** and the photographs of the dispersions are shown in **Figure 4**. Stable SWCNT dispersions were formed in **P4**/CG100, **P4**/HiPCO and **P4**/SG65i as well-resolved absorption peaks were observed in S_{11}, S_{22} and M_{11} regions. Similarly, the non-covalent binding of **P4** to the SWCNTs is confirmed by the minimal change in I_D/I_G (**Figure S6–7**). For CarboLex, which comprises SWCNTs with diameters larger than the pentiptycene cleft size, the supernatant color is close to that of pure **P4**, consistent with the UV-Vis-NIR spectrum which indicates that minimal amount of CarboLex SWCNTs are dispersed.

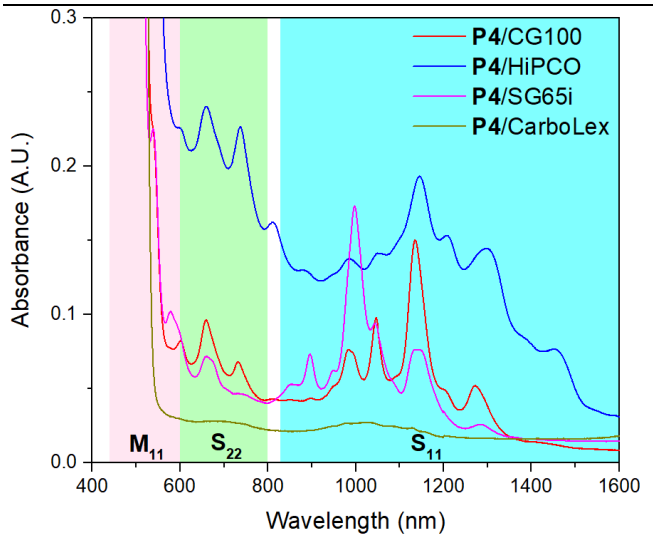

Figure 3. UV−vis−NIR absorption spectra of supernates of **P4**/HiPCO (blue), **P4**/CG100 (red), **P4**/SG65i (purple) and **P4**/CarboLex (orange). The pink, green and cyan boxes indicate the locations of optical transitions of metallic (M_{11}) and semiconducting (S_{22}, S_{11}) SWCNTs, respectively.

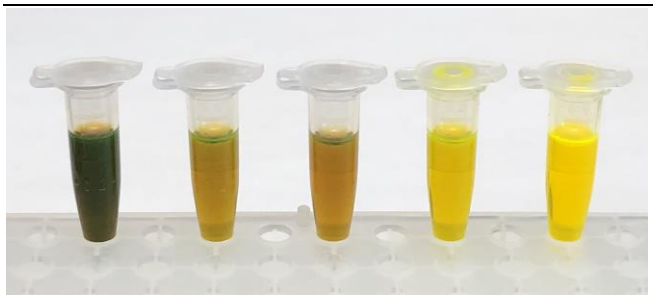

Figure 4. Photographs of supernates of **P4**/HiPCO, **P4**/CG100, **P4**/SG65i, **P4**/CarboLex and **P4** solution in chlorobenzene (from left to right).

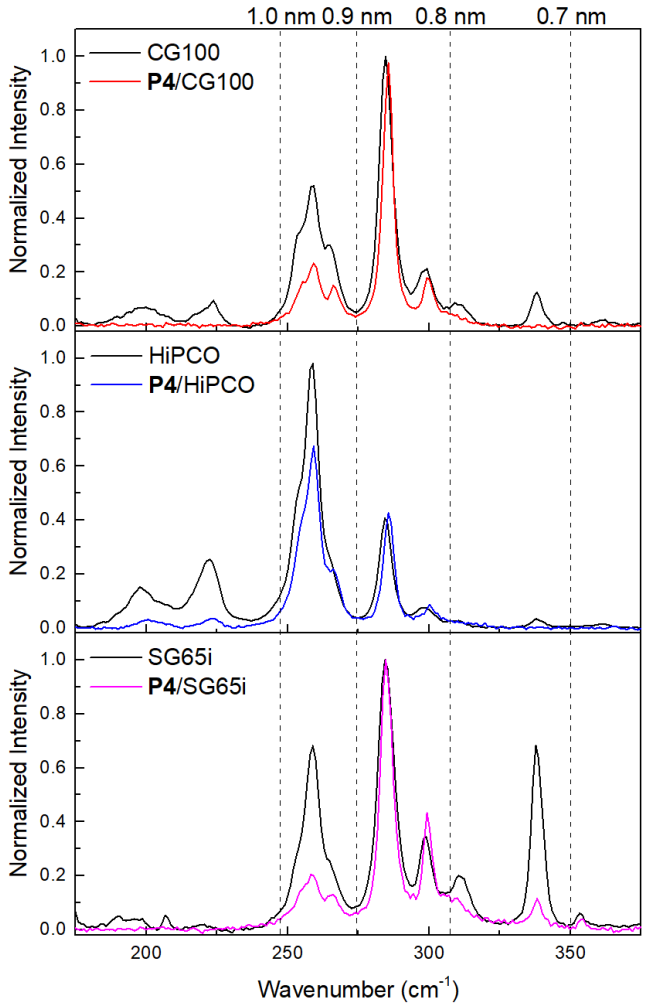

Figure 5. Radial breathing mode (RBM) region of the Raman spectra of pristine SWCNTs and **P4**/SWCNT dispersions normalized to the peak at 285 cm^{-1} (excitation at 633 nm). Dotted lines indicate the estimated SWCNT diameter.

Central to our proposed SWCNT binding model is the diameter selectivity provided by the pentiptycene unit towards a range of SWCNTs. Raman radial breathing mode (RBM) of pristine SWCNT and the polymer/SWCNT complexes, which correlates strongly with SWCNT diameter,[73–77] are evaluated in **Figure 5**. Raman intensities are normalized to the peak at 285 cm^{-1} to illustrate the relative change in the SWCNT diameter distribution. The estimated SWCNT diameters are indicated by the dotted

lines following a reported equation.[74] As shown in **Figure 5**, SWCNTs with diameters larger than 1.0 nm or smaller than 0.8 nm are significantly reduced after polymer dispersion. An enrichment of SWCNTs with 0.8–0.9 nm diameters were observed for all dispersions, matching the cleft size of the pentiptycene unit which facilitates the strong polymer-SWCNT interaction. It should also be noted that the RBM as well as the G-band peaks of the polymer/SWCNT complexes are shifted from their counterparts in pristine SWCNTs (**Figure 5, S8**), which suggest effective binding of the polymer on the surface of SWCNTs.[73–77] Moreover, the binding of the polymers to the SWCNTs is also apparent from the excited state electron and/or energy transfer that leads to fluorescence quenching. As shown in **Figure 6**, the emission intensities of **P4**/SWCNT complexes were found to be attenuated by 60−80% comparing to the pure **P4** solution at the same concentration. Emission peaks of **P4**/SWCNT dispersions agree with that of neat **P4** solution, indicating no significant polymer scission from the tip sonication procedure, which is also supported by the UV-Vis-NIR absorption comparison (**Figure S10**).

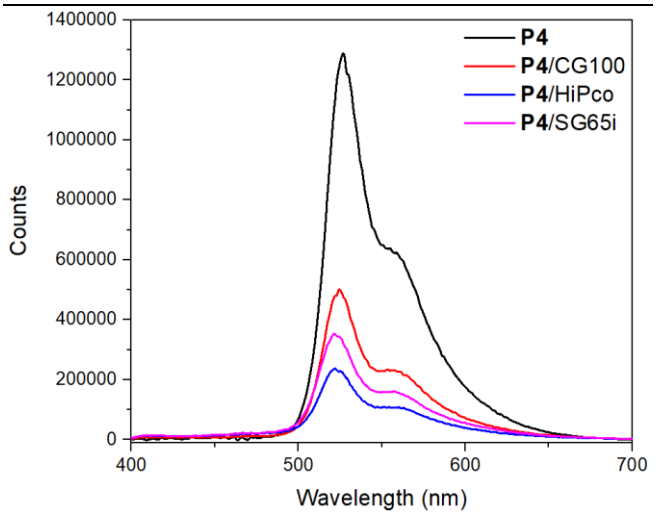

Figure 6. Emission spectra (λ_{ex} = 350 nm) of supernates of **P4**/CG100 (red), **P4**/HiPCO (blue), **P4**/SG65i (purple) and **P4** solution (black) in chlorobenzene. The polymer concentration is 0.75 mg/mL in all cases.

TEM images of dropcast films of **P1**/SG65i, **P2**/SG65i and **P4**/SG65i are shown in **Figure 7**. The linear structures observed are consistent with aligned networks of SWCNT/polymer aggregates. The parallel red lines in the inset highlights the periodic fringes of SWCNTs, which have a center-to-center distance of ~3 nm (**Figure S11**–**S12**). This gives an intertube distance of ~2.2nm that is significantly larger than the intertube distance in SWCNT bundles determined previously.[78–80] The increased intertube spacing is consistent with the presence of pentiptycene dispersing polymers between the tubes as shown schematically in **Figure 8**. This model is consistent with the 1 nm diameter of pentiptycene clefts and that dispersed SWCNTs will have polymers bound to their surface, consistent with previous reports where PPEs are shown to stack directly on the SWCNT surface by AFM and TEM studies.[55,56] Hence, in the film there are on average two polymer chains between each SWCNT, which creates molecularly defined cavities in the films.

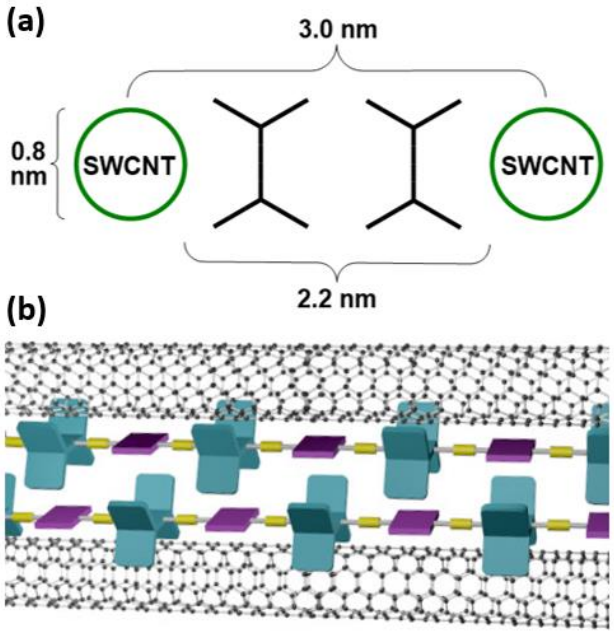

Figure 8. Schematic drawing of pentiptycene polymer/SWCNT composition in dropcast film

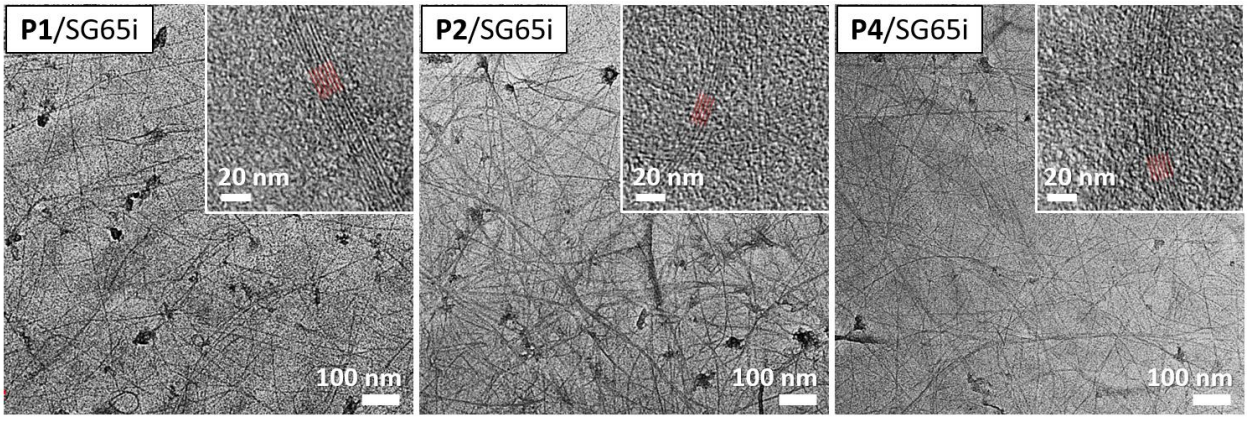

Figure 7. TEM images of dropcast films of **P1**/SG65i (left), **P2**/SG65i (middle) and **P4**/SG65i (right). Inset figures are at higher magnification. Inset figures are at higher magnification which show periodic fringes of SWCNTs.

The porous structures with high aspect ratio galleries created by the polymer/SWCNT complexes presents an opportunity to detect volatile organic vapors. Considering the planar nature of the comonomers in the pentiptycene polymers, we have evaluated their efficacy for interacting with the planar aromatic organics: benzene, toluene, and xylenes (BTX). Detection of BTX is of interest in environmental health and safety as a result of their toxicity. The parallel bundles of polymer/SWCNT observed in our TEM studies suggest that these composites may create interstitial galleries that can differentiate vapors based on size-exclusion. The diffusion of aromatic vapors into these galleries is expected to swell the polymer/SWCNT structures and thereby induce the changes of conductance. (6,5)-enriched SWCNTs SG65i were used to fabricate the sensors with revised procedures as a result of their high semiconducting content which has been shown to aid sensing sensitivity.[51,81] Devices were prepared by drop-casting polymer/SWCNT supernates (1 μL) on gold electrodes with an interelectrode spacing of 1 mm, followed by drying *in vacuo*. The change in resistance resulting from the exposure to the analyte vapor was converted to the negative normalized change in conductance, $-\Delta G/G_0$, where ΔG and G_0 are the change in conductance and baseline conductance, respectively. **Figure 9** summarizes the chemiresistive responses ($-\Delta G/G_0$) of pristine SG65i, **P1**/SG65i, **P2**/SG65i and **P4**/SG65i with exposures to benzene, toluene, and *o*-xylene (100 ppm) for 1 min in air. Minor baseline correction was applied to account for the linear drift of the baseline conductance.

As shown in **Figure 9**, films of pristine SG65i show very weak responses to BTX vapor. For **P1**/SG65i, the averaged response toward 100 ppm benzene vapor is about 0.15% with an excellent signal-to-background ratio and is approximately 2X more sensitive than our previous BTX chemiresistive sensors.[82] For **P2**/SG65i and **P4**/SG65i, the responses to benzene vapor (~0.25%) are higher than that of **P1**/SG65i, while maintaining high signal-to-noise ratios. Exposure to toluene and *o*-xylene vapors results in much higher signals across all sensors. The averaged sensor responses of **P1**/SG65i, **P2**/SG65i and **P4**/SG65i to 100 ppm toluene vapor in air are about 0.8%, 1.2% and 1.5%, respectively. For exposure of 100 ppm *o*-xylene vapor in air, the averaged sensor responses of **P1**/SG65i, **P2**/SG65i and **P4**/SG65i are about 1.1%, 1.7% and 1.9%, respectively. Notably, the sensing responses towards BTX vapors are highly reversible with small variations across different fabricated devices and are equivalent in dry air or nitrogen (**Figure S13**). The sensing performance is largely maintained at relatively high humidity of 50–70% (**Figure S14**). Together, these results confirm the utility and robustness of these sensory materials in BTX detection.

It is worth noting that the resistance of the devices fabricated from similar amounts of different polymer/SWCNT dispersions varies greatly from ~20 kΩ (**P1**/SG65i) to ~1 MΩ (**P4**/SG65i). We believe this is also indicative of the quality of the polymer/SWCNT dispersions and better dispersions will restrict direct SWCNT/SWCNT interactions and thereby lead to high resistivity. The well-resolved absorption spectrum (**Figure 3**) and the attenuated emission intensity (**Figure 6**) of **P4**/SG65i supports that SWCNTs are well dispersed and tight binding to **P4** creates molecular insulation on individual tubes. For all sensors, the responses toward benzene and toluene are extremely rapid with a "step-function" type profile that saturates within 10 sec and returns to the baseline within 1 min after the exposure. This indicates that the gas molecules diffuse into and out of binding sites quickly. The conductance profile for *o*-xylene sensing has more sluggish kinetics which is consistent with its bulkier structure. It should be noted that the BTX molecules have similar electronic and structural properties. The differences in the temporal responses can potentially be used to differentiate between analytes.

We are particularly interested in detecting benzene, which is a challenging important target in chemical sensing. **Figure 10a** illustrates the responses of the sensors fabricated from **P4**/SG65i dispersion towards benzene vapor at different concentrations in air for 1 min. These results show that we can reproducibly detect benzene down to 5 ppm (**Figure 10a**, inset), which is at the OSHA short-term exposure limit.[83] Similarly, clear signals were observed for all our sensors at 5 ppm of benzene (**Figure S15**), highlighting the potential utility in real-word benzene monitoring. As summarized in **Figure 10b**, sensors fabricated from **P4**/SG65i perform the best with the strongest responses towards benzene at concentrations ranging from 5 to 450 ppm compared to **P1**/SG65i and **P2**/SG65i. The change of chemiresistance is proportional to benzene concentration with high linear relationships ($R^2 > 0.997$). The limit of detection (LOD) was calculated to be 4, 3 and 3 ppm for **P1**/SG65i, **P2**/SG65i and **P4**/SG65i, respectively.

Figure 11 summarizes the selectivity of our sensors when challenged against various volatile organic compounds (VOCs) at 100 ppm in dry air. Overall, the sensors exhibit excellent selectivity towards BTX compared to common VOCs that give 0.15% responses at the same concentrations. Notably, the responses toward vapor of cyclohexane, the alkyl analogue to benzene, are only half of the responses towards benzene vapors. Moreover, the SWCNTs, which are naturally *p*-doped generally have higher responses to polar molecules, but in this case the non-polar BTX analytes have higher responses. These observations confirm the importance of the aromatic pentiptycene polymers for selective BTX sensing *via* structural recognition and π–π interactions.

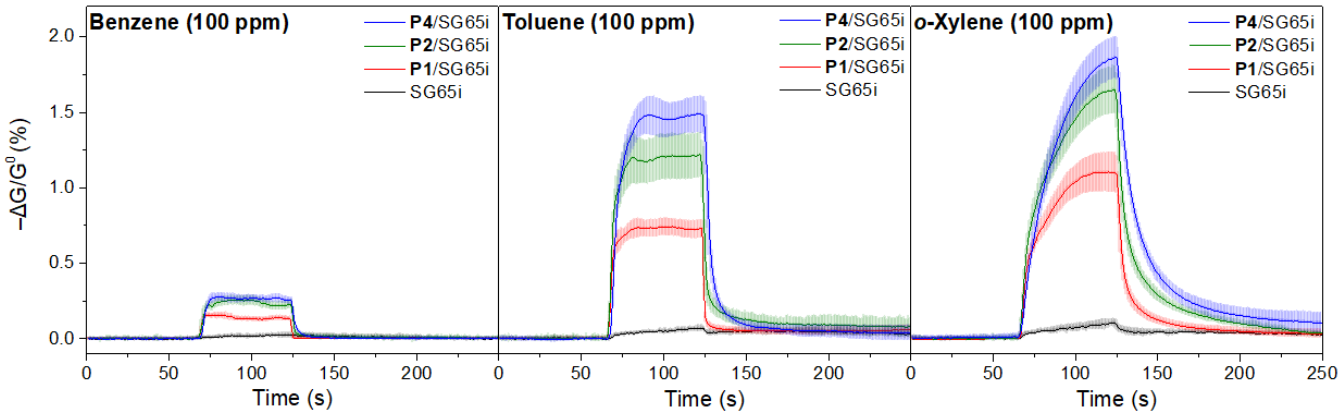

Figure 9. Chemiresistive responses of pristine SG65i (black), **P1**/SG65i (red), **P2**/SG65i (green) and **P4**/SG65i (blue) in response to benzene (left), toluene (middle) and *o*-xylene (right) in air. Devices were exposed to analyte at 100 ppm in air for 1 min (N ≥ 6).

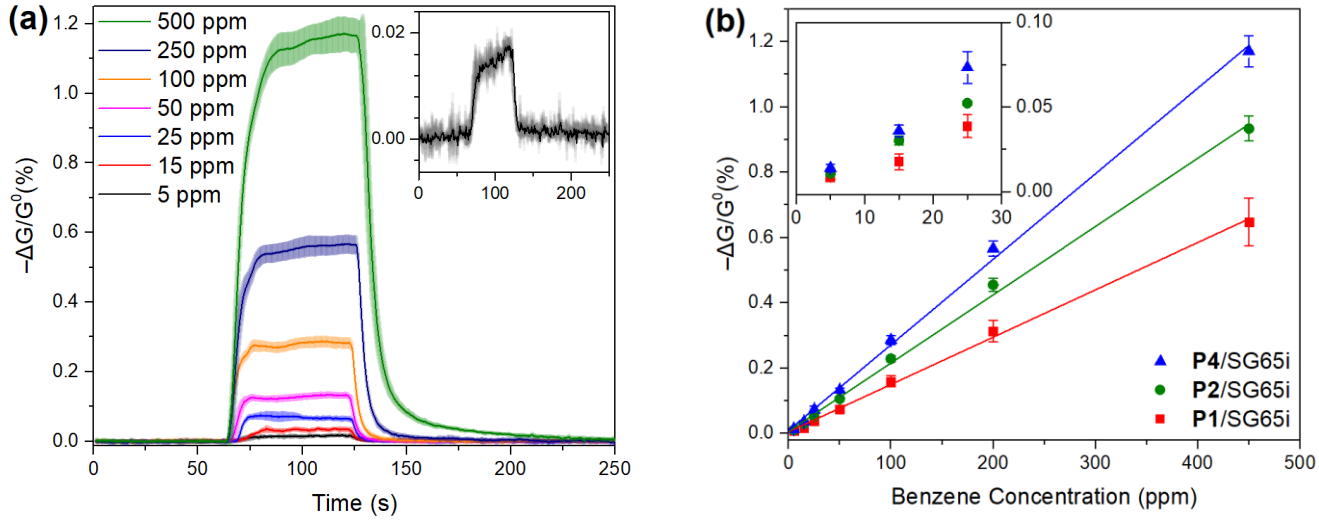

Figure 10. (a) Chemiresistive responses of **P4**/SG65i at different concentrations of benzene. The enlarged responses to benzene vapor at 5 ppm are shown in inlet. (b) Summary of chemiresistive responses of **P1**/SG65i (red), **P2**/SG65i (green) and **P4**/SG65i (blue) at different concentrations of benzene. Devices were exposed to benzene in dry air for 1 min (N ≥ 6).

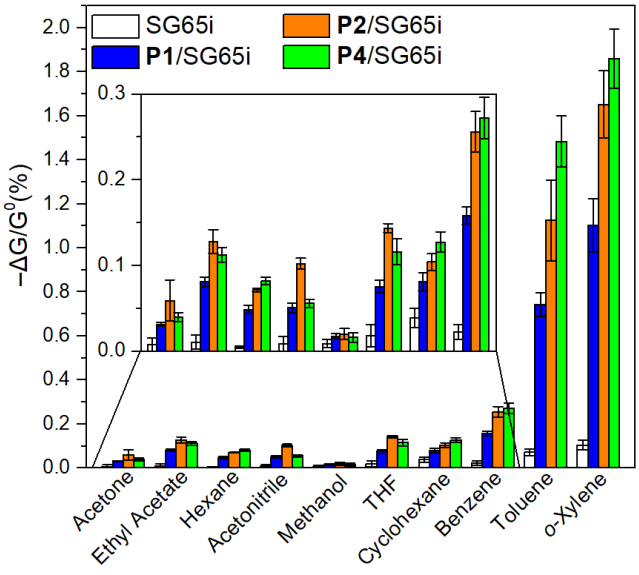

Figure 11. Chemiresistive responses of pristine SG65i (white), **P1**/SG65i (blue), **P2**/SG65i (orange) and **P4**/SG65i (green) in response to different volatile organic vapors. Devices were exposed to analyte at 100 ppm in dry air for 1 min (N ≥ 6).

To further access the binding of BTX molecules to the polymer/SWCNT composites, we have performed sensing experiments using a quartz crystal microbalance with dissipation monitoring (QCM-D). Polymer/SWCNT supernates (5 μL) were drop-casted on the gold coating of QCM-D electrodes, followed by drying *in vacuo*. The sensing responses are represented by the changes in the 3rd overtone of frequency (ΔF_3) and the dissipation factor (ΔD_3) over three cycles of analyte exposures.[82] Representative sensing profiles of **P1**/SG65i-coated electrodes towards BTX vapors at 100 ppm in air are shown in **Figure 12**. As expected, the binding of analyte molecules to the electrode surfaces result in an increase in mass and thus a decrease in frequency. The increase in the dissipation factor indicates the change in the viscoelastic properties induced by the binding of guest molecules to the surface of the **P1**/SG65i-coated electrode. It should be noted that the structural assemblies of

the polymer/SWCNT complexes are found to aid BTX binding as the polymer/SWCNT-coated electrodes exhibit significantly higher change in frequency upon the exposure of BTX vapors than pure polymer-coated or uncoated electrodes (**Figure S16–S18**). The magnitude of ΔF_3 and ΔD_3 are in the order of *o*-xylene > toluene > benzene which is consistent with the chemiresistance sensing results. Moreover, as summarized in **Figure 13a**, **S19a** and **S20a**, the sensors exhibit linear response ($R^2 > 0.993$) for BTX vapors within the range of 100–1500, 100–1000 and 100–500 ppm, respectively. These results showcase the feasibility of BTX sensing by the polymer/SWCNT complexes with QCM-D.

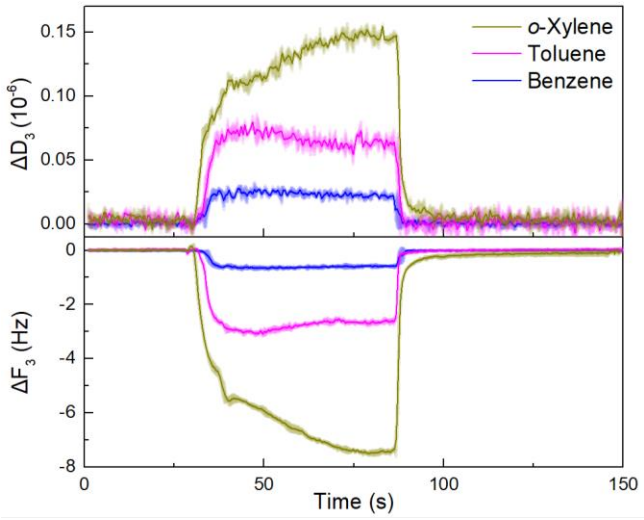

Figure 12. Changes in frequency (ΔF_3, 3rd overtone) and dissipation factor (ΔD_3, 3rd overtone) of **P1**/SG65i-coated electrode upon three cycles of exposure to BTX vapors at 100 ppm for 1 min in air.

In order to differentiate the signals between BTX vapors, we herein make use of a characteristic value derived from $-\Delta F_3/\Delta D_3$,[84] which has been used to study the contact mechanics of biomolecules,[85] microbes[86–88] and nanomaterials[89,90] with substrate surfaces. As illustrated in **Figure 13a**, the absolute magnitudes of ΔF_3 and ΔD_3 of the **P1**/SG65i-coated electrode increases with rising analyte concentration. However, the values of $-\Delta F_3/\Delta D_3$ shown in **Figure 13b** remain nearly constant over the dynamic range of the sensor. The values of $-\Delta F_3/\Delta D_3$ obtained from the BTX exposures are significantly different, with the order of *o*-xylene > toluene > benzene; they have been found to correlate with the molecular weight of the analytes.[91,92] Gratifyingly, we have observed the similar BTX differentiation by the values of $-\Delta F_3/\Delta D_3$ in other sensors made from **P2**/SG65i and **P4**/SG65i (**Figure S19b** and **S20b**). Therefore, with the ability to differentiate BTX molecules, the QCM-D method can complement chemiresistance-based sensing for the sensitive and selective detection of BTX vapors. This illustrates opportunities for the introduction of additional functionality to the pentiptycene polymer/SWCNT complexes in future sensor design to robustly detect and differentiate more complex analytes.

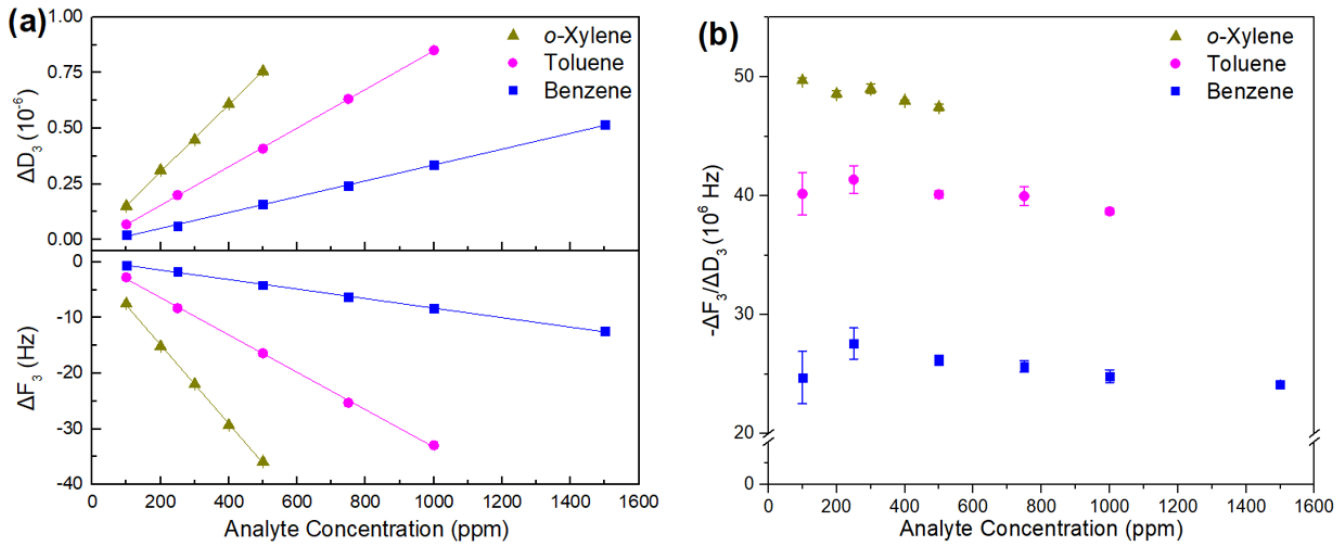

Figure 13. (a) Summary of changes in frequency (ΔF_3, 3rd overtone) and dissipation factor (ΔD_3, 3rd overtone) of **P1**/SG65i-coated electrode upon three cycles of exposure to analyte at different concentrations for 1 min in air. (b) Summary of $-\Delta F_3/\Delta D_3$ of **P1**/SG65i-coated electrode upon three cycles of exposure to analyte at different concentrations for 1 min in air.

CONCLUSION

We have developed polymer/SWCNT dispersions and thin film compositions that use the clefts of pentiptycene groups to bind the nanotubes. Strong π–π interactions between polymers and SWCNTs are found to require a complementary "fit" between the nanotube and the pentiptycene. TEM results support a structural model wherein SWCNTs bind polymers coincidently with their long axis, which provides for free volume between the tubes. The quality of dispersions is evidenced by UV-Vis-NIR absorption spectra and the minimal perturbation to the SWCNT electronic structure in the dispersion was confirmed

by Raman spectroscopy. The polymer construction allows for the robust and selective detection of BTX vapors in air by monitoring the change of conductance, QCM frequency, and the dissipation factor. Notably, our sensors are sensitive enough to detect benzene at the OSHA short-term exposure limit. In total, we have demonstrated that pentiptycene groups can create defined structural assemblies with SWCNTs and will be working to develop functional materials by extending this supramolecular model.

EXPERIMENTAL

Materials. Commercial reagents were purchased from Sigma-Aldrich, Alfa Aesar, and TCI and used as received unless otherwise noted. Deuterated solvents were purchased from Cambridge Isotope Laboratories and used as received. CoMoCAT single-walled carbon nanotubes [Signis CG100, lot #: MKBP3333V; carbon ≥ 90%; ≥ 70% carbon as SWNT; 0.7–1.3 nm diameter], (6,5)-enriched single-walled carbon nanotubes [Signis SG65i, lot #: MKBZ1159V; (6,5) chirality, ≥ 93 % carbon as SWCNT; 0.7–0.9 nm diameter] and arc discharge single-walled carbon nanotubes [CarboLex AP-grade lot #: 07826BA; 50%–70% carbon basis; 1.2–1.5 nm diameter] were purchased from Sigma-Aldrich and used as received. HiPCO single-walled carbon nanotubes [lot #: P0261, 0.8–1.2 nm diameter] were purchased from Unidym Inc. and used as received.

Instrument. NMR spectra were recorded using a Bruker Avance 400 MHz NMR or JEOL 500 MHz spectrometer. Tip sonication was performed with Qsonica Q125 Sonicator. Absorption spectra were obtained using an Agilent Cary 4000 UV-Vis-NIR spectrophotometer. Photoluminescence and excitation spectra were acquired on a HORIBA Jobin Yvon Fluorolog-3 spectrofluorometer (model FL-321) equipped with a 450 W Xenon lamp as the excitation source and a F-3000 Fiber Optic Mount that allows for fluorescence imaging outside of the sample compartment. The F-3000 couples to the T-box; light is focused from the excitation spectrometer onto the fiber-optic bundle, and then directed to the sample. Fluorescence emission from the sample is directed back through the bundle and into the front-face collection port in the sample compartment. Polymer/SWCNT supernates after centrifuge were deposited into a short-path-length cell from Starna for the collection of the absorption spectra. Raman spectra were collected using a Horiba Jobin-Yvon LabRam (Model HR 800) Raman confocal microscope with a 633 nm laser (1.4 μm spot size). Laser intensity was set to 10% for the 633 nm excitation wavelength. Analyte gases were generated by a FlexStream™ FlexBase Module with precise temperature (±0.01 °C) and gas flow rate control (±1.5% of the reading). Resistance was measured using an Agilent Keysight 34970A potentiostat equipped with a 34901A 20-channel multiplexer (2/4-wire) module. The potentiostat was connected to the sensing laptop using an Agilent 82357B GPIB-USB Interface High-Speed USB 2.0 serial cable and controlled using BenchLink Data Logger 3 (available free of charge online). The scan rate was set to 1 scan/second. Quartz crystal microbalance with dissipation monitoring (QCM-D) experiments were performed using Q-Sense E1 (Q-Sense, Stockholm, Sweden) with gold-coated AT-cut quartz crystal sensors (QSX 301 Gold, Q-Sense, Stockholm, Sweden) with 5 MHz fundamental resonance frequency.

Synthesis of polymer. 2-octyldodecan-1-amine,[93] and pentiptycene diacetylene[64] were synthesized according to methods previously reported. The synthesis of polymer **P2**,[64] **P3**,[94] **P4**[95] and **P5**[3] were reported by our group. **P1** was synthesized through Sonogashira reaction: under a nitrogen atmosphere, pentiptycene diacetylene (1.0 equiv), dibromonaphthalene diimide (1.0 equiv), $Pd(PPh_3)_4$ (10 mol%), and CuI (0.5 equiv) were dissolved in a previously degassed mixture of dry toluene and diisopropylamine. The solution was heated at 70 °C for 3 days and then subjected to a $CHCl_3/H_2O$ workup. The combined organic phase was washed with $NH_4Cl(aq)$ and dried by $MgSO_4$. The solvent was removed *in vacuo* and the residue was precipitated in methanol three times. GPC (THF *vs.* PS): Mn = 25100, Mw = 42700, PDI = 1.70.

Preparation of polymer/SWCNT dispersion. Polymer (3 mg) was dissolved in chlorobenzene (4 mL) and the solution was sonicated in water bath for 10 mins. To the polymer solution, 2 mg of SWCNT was added and the resulting mixture was chilled with ice and homogenized for 30 mins using Qsonica Q125 Sonicator at 63W. Subsequently, the suspension was centrifuged for 4 hours at 30130 g. For UV-Vis-NIR absorption spectroscopy and photoluminescence spectroscopy, the absorption and the emission spectra of supernatant were directly recorded in a 1 mm short-path path quartz cuvette.

Chemiresistive device preparation. Glass slides (VWR microscope slides) were bath sonicated in acetone for 15 min and then dried with a stream of nitrogen. Using an aluminum mask, chromium (15 nm) followed by gold (50 nm) was deposited using a Thermal Evaporator (Angstrom Engineering), leaving a 1 mm gap between gold electrodes. **For pristine SG65i SWCNTs:** A stock solution of SG65i SWCNTs (2 mg) was prepared in *o*-dichlorobenzene (*o*DCB) (20 mL) by bath sonication at RT for 30 min. 1 μL of the SG65i SWCNT dispersion was drop-casted in between the gold electrodes and dried at RT under house vacuum in a desiccator or vacuum oven. **For polymer/SWCNT dispersions:** Polymer (10 mg) was dissolved in *o*-dichlorobenzene (*o*DCB, 10 mL) and the solution was sonicated in water bath for 10 mins. To the polymer solution, 1 mg of SG65i SWCNT was added and the resulting mixture was chilled with ice and homogenized for 20 mins using Qsonica Q125 Sonicator at 63W. Subsequently, the suspension was centrifuged for 30 min at 8000 g and allowed to stand overnight undisturbed. 1 μL of the polymer/SWCNT supernate was drop-casted in between the gold electrodes and dried at RT under house vacuum in a desiccator or vacuum oven.

TEM imaging. The polymer/SWCNT supernates prepared for sensing was diluted by *o*DCB 10 times. The solution (~10 μL) was then drop-casted onto the TEM grid (Lacey C only) and dried to evaporate all *o*DCB at room temperature.

Analyte gas generation. A gas generator (FlexStream, Kin-Tek) is used to produce gas vapors from liquid sources. A trace amount of analyte is emitted from a permeation tube diluted in air, which is further diluted with air to adjust the concentration (in ppm) of analyte. BTX and VOCs were calibrated by placing 2–3 mL of the liquid in the oven flow and measuring the mass loss after a known length of time at a constant temperature.

Chemiresistive gas sensing measurements. Chemiresistive device was enclosed in a homemade Teflon gas flow chamber. The resistance of the device was measured over time (1 scan/sec), with typical procedures including 5 min equilibration time (for the baseline resistance to stabilize) followed by 1 min exposure to analyte in air and then 5 min of recovery. All presented data are given as the numeral average ($N \geq 6$) accompanied by the standard deviation.

Quartz crystal microbalance with dissipation monitoring (QCM-D) gas sensing experiments. Polymer solution or Polymer/SWCNT supernatant (5 μL) was drop-casted on the gold coating of QCM-D electrodes, followed by drying *in vacuo*. The 3rd overtone of frequency (ΔF_3) and the dissipation factor (ΔD_3) of a film on a QCM sensor was measured by three cycles of exposure of a film to an analyte vapor for 1 min at 23 °C. Typical procedures include 5 min equilibration time followed by 1 min exposure to analyte in air and then 5 min of recovery.

ASSOCIATED CONTENT

Supporting Information

Photophysical studies; additional sensing results; NMR spectra of **P1**. This material is available free of charge at http://pubs.acs.org.

A patent has been filed on this technology.

AUTHOR INFORMATION

Corresponding Author

*tswager@mit.edu

Present Addresses

§ Department of Chemistry, National Dong Hwa University, Hualien 97401, Taiwan

Author Contributions

†These authors contributed equally.

ACKNOWLEDGEMENT

This work was supported by the National Institute of Environmental Health Sciences Superfund Basic Research Program, National Institute of Health, P42 ES027707 and the National Science Foundation DMR-1809740. We thank Dr. Darryl Fong, Dr. Ruqiang Lu and Prof. Maggie He for insightful discussions.

REFERENCES

(1) Kauffman, D. R.; Star, A., Carbon Nanotube Gas and Vapor Sensors. *Angew. Chem., Int. Ed.* **2008**, *47*, 6550−6570.

(2) Fennell, J. F.; Liu, S. F.; Azzarelli, J. M.; Weis, J. G.; Rochat, S.; Mirica, K. A.; Ravnsbæk, J. B.; Swager, T. M., Nanowire Chemical/Biological Sensors: Status and a Roadmap for the Future. *Angew. Chem., Int. Ed.* **2015**, *55*, 1266−1281.

(3) Star, A.; Joshi, V.; Skarupo, S.; Thomas, D.; Gabriel, J.-C. P., Gas Sensor Array Based on Metal-Decorated Carbon Nanotubes. *J. Phys. Chem. B* **2006,** *110*, 21014−21020.

(4) Meyyappan, M., Carbon Nanotube-Based Chemical Sensors. *Small* **2016**, *12*, 2118−2129.

(5) Schroeder, V.; Savagatrup, S.; He, M.; Lin, S.; Swager, T. M., Carbon Nanotube Chemical Sensors. *Chem. Rev.* **2019**, *119*, 599−663.

(6) He, M.; Swager, T. M., Covalent Functionalization of Carbon Nanomaterials with Iodonium Salts. *Chem. Mater.* **2016**, *28*, 8542−8549.

(7) Sakellariou, G.; Priftis, D.; Baskaran, D., Surface-Initiated Polymerization from Carbon Nanotubes: Strategies and Perspectives. *Chem. Soc. Rev.* **2013**, *42*, 677−704.

(8) Schnorr, J. M.; Zwaag, D. v. d.; Walish, J. J.; Weizmann, Y.; Swager, T. M., Sensory Arrays of Covalently Functionalized Single-Walled Carbon Nanotubes for Explosive Detection. *Adv. Funct. Mater.* **2013**, *23*, 5285−5291.

(9) Paoletti, C.; He, M.; Salvo, P.; Melai, B.; Calisi, N.; Mannini, M.; Cortigiani, B.; Bellagambi, F. G.; Swager, T. M.; Di Francesco, F.; Pucci, A., Room Temperature Amine Sensors Enabled by Sidewall Functionalization of Single-Walled Carbon Nanotubes. *RSC Adv.* **2018**, *8*, 5578−5585.

(10) Fong, D.; Andrews, G. M.; McNelles, S. A.; Adronov, A., Decoration of Polyfluorene-Wrapped Carbon Nanotube Thin Films *via* Strain-Promoted Azide–Alkyne Cycloaddition. *Polym. Chem.* **2018**, *9*, 4460−4467.

(11) Fong, D.; Andrews, G. M.; Adronov, A., Functionalization of Polyfluorene-Wrapped Carbon Nanotubes *via* Copper-Mediated Azide–Alkyne Cycloaddition. *Polym. Chem.* **2018**, *9*, 2873−2879.

(12) Zeininger, L.; He, M.; Hobson, S. T.; Swager, T. M., Resistive and Capacitive γ-Ray Dosimeters Based On Triggered Depolymerization in Carbon Nanotube Composites. *ACS Sens.* **2018**, *3*, 976−983.

(13) Fennell, J. F.; Hamaguchi, H.; Yoon, B.; Swager, T. M., Chemiresistor Devices for Chemical Warfare Agent Detection Based on Polymer Wrapped Single-Walled Carbon Nanotubes. *Sensors* **2017**, *17*, 982.

(14) Fong, D.; Yeung, J.; McNelles, S. A.; Adronov, A., Decoration of Polyfluorene-Wrapped Carbon Nanotubes *via* Strain-Promoted Azide–Alkyne Cycloaddition. *Macromolecules* **2018**, *51*, 755−762.

(15) Bilalis, P.; Katsigiannopoulos, D.; Avgeropoulos, A.; Sakellariou, G., Non-Covalent Functionalization of Carbon Nanotubes with Polymers. *RSC Adv.* **2014**, *4*, 2911−2934.

(16) Wei, L.; Lu, D.; Wang, J.; Wei, H.; Zhao, J.; Geng, H.; Zhang, Y., Highly Sensitive Detection of Trinitrotoluene in Water by Chemiresistive Sensor Based on Noncovalently Amino Functionalized Single-Walled Carbon Nanotube. *Sens. Actuators, B* **2014**, *190*, 529−534.

(17) Zhao, Y.-L.; Hu, L.; Stoddart, J. F.; Grüner, G., Pyrenecyclodextrin-Decorated Single-Walled Carbon Nanotube Field-Effect Transistors as Chemical Sensors. *Adv. Mater.* **2008**, *20*, 1910−1915.
(18) Lerner, M. B.; Kybert, N.; Mendoza, R.; Villechenon, R.; Lopez, M. A. B.; Johnson, A. T. C., Scalable, Non-Invasive Glucose Sensor Based on Boronic Acid Functionalized Carbon Nanotube Transistors. *Appl. Phys. Lett.* **2013**, *102*, 183113.
(19) Frazier, K. M.; Swager, T. M., Robust Cyclohexanone Selective Chemiresistors Based on Single-Walled Carbon Nanotubes. *Anal. Chem.* **2013**, *85*, 7154−7158.
(20) Zhu, R.; Azzarelli, J. M.; Swager, T. M., Wireless Hazard Badges to Detect Nerve-Agent Simulants. *Angew. Chem., Int. Ed.* **2016**, *55*, 9662−9666.
(21) Weis, J. G.; Ravnsbæk, J. B.; Mirica, K. A.; Swager, T. M., Employing Halogen Bonding Interactions in Chemiresistive Gas Sensors. *ACS Sens.* **2016**, *1*, 115−119.
(22) Liu, S. F.; Petty, A. R.; Sazama, G. T.; Swager, T. M., Single-Walled Carbon Nanotube/Metalloporphyrin Composites for the Chemiresistive Detection of Amines and Meat Spoilage. *Angew. Chem., Int. Ed.* **2015**, *54*, 6554−6557.
(23) Liu, S. F.; Lin, S.; Swager, T. M., An Organocobalt-Carbon Nanotube Chemiresistive Carbon Monoxide Detector. *ACS Sens.* **2016**, *1*, 354−357.
(24) Esser, B.; Schnorr, J. M.; Swager, T. M., Selective Detection of Ethylene Gas Using Carbon Nanotube-Based Devices: Utility in Determination of Fruit Ripeness. *Angew. Chem., Int. Ed.* **2012**, *51*, 5752−5756.
(25) Chen, R. J.; Bangsaruntip, S.; Drouvalakis, K. A.; Wong Shi Kam, N.; Shim, M.; Li, Y.; Kim, W.; Utz, P. J.; Dai, H., Noncovalent Functionalization of Carbon Nanotubes for Highly Specific Electronic Biosensors. *Proc. Natl. Acad. Sci. U. S. A.* **2003**, *100*, 4984−4989.
(26) O'Connell, M. J.; Boul, P.; Ericson, L. M.; Huffman, C.; Wang, Y.; Haroz, E.; Kuper, C.; Tour, J.; Ausman, K. D.; Smalley, R. E. Reversible Water-Solubilization of Single-Walled Carbon Nanotubes by Polymer Wrapping. *Chem. Phys. Lett.* **2001**, *342*, 265−271.
(27) Fong, D.; Adronov, A. Recent Developments in the Selective Dispersion of Single-Walled Carbon Nanotubes Using Conjugated Polymers. *Chem. Sci.* **2017**, *8*, 7292−7305.
(28) Llanes-Pallas, A.; Yoosaf, K.; Traboulsi, H.; Mohanraj, J.; Seldrum, T.; Dumont, J.; Minoia, A.; Lazzaroni, R.; Armaroli, N.; Bonifazi, D. Modular Engineering of H-Bonded Supramolecular Polymers for Reversible Functionalization of Carbon Nanotubes. *J. Am. Chem. Soc.* **2011**, *133*, 15412−15424.
(29) Nish, A.; Hwang, J.-Y.; Doig, J.; Nicholas, R. J. Highly Selective Dispersion of Single-Walled Carbon Nanotubes Using Aromatic Polymers. *Nat. Nanotechnol.* **2007**, *2*, 640−646.
(30) Hwang, J. Y.; Nish, A.; Doig, J.; Douven, S.; Chen, C. W.; Chen, L. C.; Nicholas, R. J. Polymer Structure and Solvent Effects on the Selective Dispersion of Single-Walled Carbon Nanotubes. *J. Am. Chem. Soc.* **2008**, *130*, 3543−3553.
(31) Chen, R. J.; Zhang, Y.; Wang, D.; Dai, H., Noncovalent Sidewall Functionalization of Single-Walled Carbon Nanotubes for Protein Immobilization. *J. Am. Chem. Soc.* **2001**, *123* , 3838−3839.
(32) Zu, S.-Z.; Sun, X.-X.; Liu, Y.; Han, B.-H. Supramolecular Surface Modification and Solubilization of Single-Walled Carbon Nanotubes with Cyclodextrin Complexation. *Chem. - Asian J.* **2009**, *4*, 1562−1572.
(33) Tromp, R. M.; Afzali, A.; Freitag, M.; Mitzi, D. B.; Chen, Z. Novel Strategy for Diameter-Selective Separation and Functionalization of Single-Wall Carbon Nanotubes. *Nano Lett.* **2008**, *8*, 469−472.
(34) Hammershøj, P.; Bomans, P. H. H.; Lakshminarayanan,R.; Fock, J.; Jensen, S. H.; Jespersen, T. S.; Brock-Nannestad, T.; Hassenkam, T.; Nygard, J.; Sommerdijk, N. A. J. M.; Kilsa, K.; Bjørnholm, T.; Christensen, J. B. A Triptycenebased Approach to Solubilising Carbon Nanotubes and C_{60}, *Chem. - Eur. J.,* **2012**, *18*, 8716−8723.
(35) Zheng, M.; Jagota, A.; Semke, E. D.; Diner, B. A.; McLean, R. S.; Lustig, S. R.; Richardson, R. E.; Tassi, N. G., DNA-Assisted Dispersion and Separation of Carbon Nanotubes. *Nat. Mater.* **2003**, *2*, 338−342.
(36) Star, A.; Joshi, V.; Han, T.-R.; Altoé, M. V. P.; Grüner, G.; Stoddart, J. F., Electronic Detection of the Enzymatic Degradation of Starch. *Org. Lett.* **2004**, *6*, 2089−2092.
(37) Star, A.; Steuerman, D. W.; Heath, J. R.; Stoddart, J. F., Starched Carbon Nanotubes. *Angew. Chem., Int. Ed.* **2002**, *41*, 2508−2512.
(38) Cella, L. N.; Chen, W.; Myung, N. V.; Mulchandani, A., Single-Walled Carbon Nanotube-Based Chemiresistive Affinity Biosensors for Small Molecules: Ultrasensitive Glucose Detection. *J. Am. Chem. Soc.* **2010**, *132*, 5024−5026.
(39) Zhang, M.; Gorski, W., Electrochemical Sensing Platform Based on the Carbon Nanotubes/Redox Mediators-Biopolymer System. *J. Am. Chem. Soc.* **2005**, *127*, 2058−2059.
(40) Star, A.; Liu, Y.; Grant, K.; Ridvan, L.; Stoddart, J. F.; Steuerman, D. W.; Diehl, M. R.; Boukai, A.; Heath, J. R., Noncovalent Side-Wall Functionalization of Single-Walled Carbon Nanotubes. *Macromolecules* **2003**, *36*, 553−560.
(41) Tang, B. Z.; Xu, H., Preparation, Alignment, and Optical Properties of Soluble Poly(phenylacetylene)-Wrapped Carbon Nanotubes. *Macromolecules* **1999**, *32*, 2569−2576.
(42) Steuerman, D. W.; Star, A.; Narizzano, R.; Choi, H.; Ries, R. S.; Nicolini, C.; Stoddart, J. F.; Heath, J. R., Interactions between Conjugated Polymers and Single-Walled Carbon Nanotubes. *J. Phys. Chem. B* **2002**, *106*, 3124−3130.
(43) Bati, A. S. R.; Yu, L.; Batmunkh, M.; Shapter, J. G., Synthesis, Purification, Properties and Characterization of Sorted Single-Walled Carbon Nanotubes. *Nanoscale* **2018,** *10*, 22087−22139.
(44) Lei, T.; Lai, Y.-C.; Hong, G.; Wang, H.; Hayoz, P.; Weitz, R. T.; Chen, C.; Dai, H.; Bao, Z. Diketopyrrolopyrrole (DPP)-Based Donor–Acceptor Polymers for Selective Dispersion of Large-Diameter Semiconducting Carbon Nanotubes. *Small* **2015**, *11*, 2946−2954.

(45) So, H.-M.; Won, K.; Kim, Y. H.; Kim, B.-K.; Ryu, B. H.; Na, P. S.; Kim, H.; Lee, J.-O., Single-Walled Carbon Nanotube Biosensors Using Aptamers as Molecular Recognition Elements. *J. Am. Chem. Soc.* **2005**, *127*, 11906−11907.
(46) Chen, F.; Wang, B.; Chen, Y.; Li, L.-J. Toward the Extraction of Single Species of Single-Walled Carbon Nanotubes Using Fluorene-Based Polymers. *Nano Lett.* **2007**, *7*, 3013−3017.
(47) Lei, T.; Pochorovski, I.; Bao, Z. Separation of Semiconducting Carbon Nanotubes for Flexible and Stretchable Electronics Using Polymer Removable Method. *Acc. Chem. Res.* **2017**, *50*, 1096−1104.
(48) Selmani, S.; Schipper, D. J., Orientation Control of Molecularly Functionalized Surfaces Applied to the Simultaneous Alignment and Sorting of Carbon Nanotubes. *Angew. Chem., Int. Ed.* **2018**, *57*, 2399−2403.
(49) Snowdon, M. R.; Selmani, S.; Schipper, D. J., Sonication-Enhanced Alignment Relay Technique for the Orientation of Single-Walled Carbon Nanotubes. *ACS Appl. Nano Mater.* **2019**, *2*, 6637−6645.
(50) Wang, F.; Gu, H.; Swager, T. M., Carbon Nanotube/Polythiophene Chemiresistive Sensors for Chemical Warfare Agents. *J. Am. Chem. Soc.* **2008**, *130*, 5392−5393.
(51) Ishihara, S.; O'Kelly, C. J.; Tanaka, T.; Kataura, H.; Labuta, J.; Shingaya, Y.; Nakayama, T.; Ohsawa, T.; Nakanishi, T.; Swager, T. M., Metallic *versus* Semiconducting SWCNT Chemiresistors: A Case for Separated SWCNTs Wrapped by a Metallosupramolecular Polymer. *ACS Appl. Mater. Interfaces* **2017**, *9*, 38062−38067.
(52) Ishihara, S.; Azzarelli, J. M.; Krikorian, M.; Swager, T. M., Ultratrace Detection of Toxic Chemicals: Triggered Disassembly of Supramolecular Nanotube Wrappers. *J. Am. Chem. Soc.* **2016**, *138*, 8221−8227.
(53) Wang, F.; Yang, Y.; Swager, T. M., Molecular Recognition for High Selectivity in Carbon Nanotube/Polythiophene Chemiresistors. *Angew. Chem., Int. Ed.* **2008**, *47*, 8394−8396.
(54) Chen, J.; Liu, H.; Weimer, W. A.; Halls, M. D.; Waldeck, D. H.; Walker, G. C., Noncovalent Engineering of Carbon Nanotube Surfaces by Rigid, Functional Conjugated Polymers. *J. Am. Chem. Soc.* **2002**, *124*, 9034−9035.
(55) Rice, N. A.; Soper, K.; Zhou, N.; Merschrod, E.; Zhao, Y., Dispersing As-Prepared Single-Walled Carbon Nanotube Powders with Linear Conjugated Polymers. *Chem. Comm.* **2006**, 4937−4939.
(56) Kang, Y. K.; Lee, O.-S.; Deria, P.; Kim, S. H.; Park, T.-H.; Bonnell, D. A.; Saven, J. G.; Therien, M. J., Helical Wrapping of Single-Walled Carbon Nanotubes by Water Soluble Poly(*p*-Phenyleneethynylene). *Nano Lett.* **2009**, *9*, 1414−1418.
(57) Chen, Y.; Xu, Y.; Wang, Q.; Gunasinghe, R. N.; Wang, X.-Q.; Pang, Y., Highly Selective Dispersion of Carbon Nanotubes by Using Poly(phenyleneethynylene)-Guided Supermolecular Assembly. *Small* **2013**, *9*, 870−875.
(58) Saem, S.; Fong, D.; Adronov, A.; Moran-Mirabal, J., Stretchable and Resilient Conductive Films on Polydimethylsiloxane from Reactive Polymer-Single-Walled Carbon Nanotube Complexes for Wearable Electronics. *ACS Appl. Nano Mater.* **2019,** *2*, 4968−4973.
(59) Yang, J.-S.; Yan, J.-L., Central-Ring Functionalization and Application of the Rigid, Aromatic, and H-Shaped Pentiptycene Scaffold. *Chem. Commun.* **2008**, 1501−1512.
(60) Lin, C.-J.; Chen, C.-Y.; Kundu, S. K.; Yang, J.-S., Unichromophoric Platinum-Acetylides That Contain Pentiptycene Scaffolds: Torsion-Induced Dual Emission and Steric Shielding of Dynamic Quenching. *Inorg. Chem.* **2014**, *53*, 737−745.
(61) Yang, J.-S.; Yan, J.-L.; Hwang, C.-Y.; Chiou, S.-Y.; Liau, K.-L.; Gavin Tsai, H.-H.; Lee, G.-H.; Peng, S.-M., Probing the Intrachain and Interchain Effects on the Fluorescence Behavior of Pentiptycene-Derived Oligo(*p*-Phenyleneethynylene)s. *J. Am. Chem. Soc.* **2006**, *128*, 14109−14119.
(62) Zhao, X.; Cardolaccia, T.; Farley, R. T.; Abboud, K. A.; Schanze, K. S., A Platinum Acetylide Polymer with Sterically Demanding Substituents: Effect of Aggregation on the Triplet Excited State. *Inorg. Chem.* **2005**, *44*, 2619−2627.
(63) Zhang, J.; Wu, N.-W.; Xu, X.-D.; Li, Q.-J.; Wang, C.-H.; Tan, H.; Xu, L., Branched Platinum–Acetylide Complexes: Synthesis, Properties, and Their Aggregation Behavior. *RSC Adv.* **2014**, *4*, 16047−16054.
(64) Yang, J.-S.; Swager, T. M., Fluorescent Porous Polymer Films as TNT Chemosensors: Electronic and Structural Effects. *J. Am. Chem. Soc.* **1998**, *120*, 11864−11873.
(65) Yang, J.-S.; Swager, T. M., Porous Shape Persistent Fluorescent Polymer Films: An Approach to TNT Sensory Materials. *J. Am. Chem. Soc.* **1998**, *120*, 5321−5322.
(66) Thomas, S. W.; Joly, G. D.; Swager, T. M., Chemical Sensors Based on Amplifying Fluorescent Conjugated Polymers. *Chem. Rev.* **2007**, *107*, 1339−1386.
(67) Lin, C.-J.; Liu, Y.-H.; Peng, S.-M.; Shinmyozu, T.; Yang, J.-S., Excimer–Monomer Photoluminescence Mechanochromism and Vapochromism of Pentiptycene-Containing Cyclometalated Platinum(II) Complexes. *Inorg. Chem.* **2017**, *56*, 4978−4989.
(68) Long, T. M.; Swager, T. M., Molecular Design of Free Volume as a Route to Low-κ Dielectric Materials. *J. Am. Chem. Soc.* **2003**, *125*, 14113−14119.
(69) Strano, M. S.; Dyke, C. A.; Usrey, M. L.; Barone, P. W.; Allen, M. J.; Shan, H.; Kittrell, C.; Hauge, R. H.; Tour, J. M.; Smalley, R. E., Electronic Structure Control of Single-Walled Carbon Nanotube Functionalization. *Science* **2003**, *301*, 1519−1522.
(70) Bachilo, S. M.; Strano, M. S.; Kittrell, C.; Hauge, R. H.; Smalley, R. E.; Weisman, R. B., Structure-Assigned Optical Spectra of Single-Walled Carbon Nanotubes. *Science* **2002**, *298*, 2361−2366.
(71) Lolli, G.; Zhang, L.; Balzano, L.; Sakulchaicharoen, N.; Tan, Y.; Resasco, D. E. Tailoring (n,m) Structure of Single-Walled Carbon Nanotubes by Modifying Reaction Conditions and the Nature of the Support of CoMo Catalysts. *J. Phys. Chem. B* **2006**, *110*, 2108−2115.
(72) Ao, G.; Streit, J. K.; Fagan, J. A.; Zheng, M., Differentiating Left- and Right-Handed Carbon Nanotubes by DNA. *J. Am. Chem. Soc.* **2016**, *138*, 16677−16685.

(73) Dresselhaus, M. S.; Dresselhaus, G.; Jorio, A.; Souza Filho, A. G.; Saito, R., Raman Spectroscopy on Isolated Single Wall Carbon Nanotubes. *Carbon* **2002**, *40*, 2043−2061.
(74) Zheng, M.; Jagota, A.; Strano, M. S.; Santos, A. P.; Barone, P.; Chou, S. G.; Diner, B. A.; Dresselhaus, M. S.; Mclean, R. S.; Onoa, G. B.; Samsonidze, G. G.; Semke, E. D.; Usrey, M.; Walls, D. J., Structure-Based Carbon Nanotube Sorting by Sequence-Dependent DNA Assembly. *Science* **2003**, *302*, 1545–1548.
(75) Chou, S. G.; Ribeiro, H. B.; Barros, E. B.; Santos, A. P.; Nezich, D.; Samsonidze, G. G.; Fantini, C.; Pimenta, M. A.; Jorio, A.; Filho, F. P.; Dresselhaus, M. S.; Dresselhaus, G.; Saito, R.; Zheng, M.; Onoa, G. B.; Semke, E. D.; Swan, A. K.; Ünlü, M. S.; Goldberg, B. B., Optical Characterization of DNA-Wrapped Carbon Nanotube Hybrids. *Chem. Phys. Lett.* **2004**, *397*, 296−301.
(76) Chen, B.; Cinke, M.; Li, J. Z.; Meyyappan, M.; Chi, Z. H.; Harmon, J. P.; Muisener, P. A. O.; Clayton, L.; D'Angelo, J., Modifying the Electronic Character of Single-Walled Carbon Nanotubes through Anisotropic Polymer Interaction: A Raman Study. *Adv. Funct. Mater.* **2005**, *15*, 1183–1187.
(77) Strano, M. S.; Zheng, M.; Jagota, A.; Onoa, G. B.; Heller, D. A.; Barone, P. W.; Usrey, M. L., Understanding the Nature of the DNA-Assisted Separation of Single-Walled Carbon Nanotubes Using Fluorescence and Raman Spectroscopy. *Nano Lett.* **2004**, *4*, 543–550.
(78) Zhang, Y.; Ichihashi, T.; Landree, E.; Nihey, F.; Iijima, S., Heterostructures of Single-Walled Carbon Nanotubes and Carbide Nanorods. *Science* **1999,** *285*, 1719.
(79) Kim, U. J.; Gutiérrez, H. R.; Kim, J. P.; Eklund, P. C., Effect of the Tube Diameter Distribution on the High-Temperature Structural Modification of Bundled Single-Walled Carbon Nanotubes. *J. Phys. Chem. B* **2005,** *109*, 23358–23365.
(80) Ramos-Sanchez, G.; Chen, G.; Harutyunyan, A. R.; Balbuena, P. B., Theoretical and Experimental Investigations of the Li Storage Capacity in Single-Walled Carbon Nanotube Bundles. *RSC Adv.* **2016,** *6*, 27260–27266.
(81) Fong, D.; Luo, S-.X.; Andre, R. S.; Swager, T. M. Trace Ethylene Sensing *via* Wacker Oxidation. *ACS Cent. Sci.* **2020**, *6*, 507−512.
(82) Im, J.; Sterner, S. E.; Swager, M. T., Integrated Gas Sensing System of SWCNT and Cellulose Polymer Concentrator for Benzene, Toluene, and Xylenes. *Sensors* **2016**, *16*, 183−195.
(83) Annotated OSHA Z-2 Table. https://www.osha.gov/dsg/annotated-pels/tablez-2.html (accessed March 1st, 2020).
(84) Huang, R.; Yi, P.; Tang, Y., Probing the Interactions of Organic Molecules, Nanomaterials, and Microbes with Solid Surfaces Using Quartz Crystal Microbalances: Methodology, Advantages, and Limitations. *Environ. Sci.: Processes Impacts* **2017**, *19*, 793−811.
(85) Gutman, J.; Kaufman, Y.; Kawahara, K.; Walker, S. L.; Freger, V.; Herzberg, M., Interactions of Glycosphingolipids and Lipopolysaccharides with Silica and Polyamide Surfaces: Adsorption and Viscoelastic Properties. *Biomacromolecules* **2014**, *15*, 2128−2137.
(86) Olsson, A. L. J.; van der Mei, H. C.; Busscher, H. J.; Sharma, P. K., Influence of Cell Surface Appendages on the Bacterium−Substratum Interface Measured Real-Time Using QCM-D. *Langmuir* **2009**, *25*, 1627−1632.
(87) Friedlander, R. S.; Vogel, N.; Aizenberg, J., Role of Flagella in Adhesion of *Escherichia coli* to Abiotic Surfaces. *Langmuir* **2015**, *31*, 6137−6144.
(88) Molino, P. J.; Hodson, O. M.; Quinn, J. F.; Wetherbee, R., The Quartz Crystal Microbalance: A New Tool for the Investigation of the Bioadhesion of Diatoms to Surfaces of Differing Surface Energies. *Langmuir* **2008**, *24*, 6730−6737.
(89) Chang, X.; Bouchard, D. C., Multiwalled Carbon Nanotube Deposition on Model Environmental Surfaces. *Environ. Sci. Technol.* **2013**, *47*, 10372−10380.
(90) Li, W.; Liu, D.; Wu, J.; Kim, C.; Fortner, J. D., Aqueous Aggregation and Surface Deposition Processes of Engineered Superparamagnetic Iron Oxide Nanoparticles for Environmental Applications. *Environ. Sci. Technol.* **2014**, *48*, 11892−11900.
(91) Speller, N. C.; Siraj, N.; McCarter, K. S.; Vaughan, S.; Warner, I. M., QCM Virtual Sensor Array: Vapor Identification and Molecular Weight Approximation. *Sens. Actuators, B* **2017**, *246*, 952−960.
(92) Regmi, B. P.; Speller, N. C.; Anderson, M. J.; Brutus, J. O.; Merid, Y.; Das, S.; El-Zahab, B.; Hayes, D. J.; Murray, K. K.; Warner, I. M., Molecular Weight Sensing Properties of Ionic Liquid-Polymer Composite Films: Theory and Experiment. *J. Mater. Chem. C* **2014**, *2*, 4867−4878.
(93) Liu, S.; Kan, Z.; Thomas, S.; Cruciani, F.; Brédas, J.-L.; Beaujuge, P. M., Thieno[3,4-*c*]pyrrole-4,6-dione-3,4-difluorothiophene Polymer Acceptors for Efficient All-Polymer Bulk Heterojunction Solar Cells. *Angew. Chem., Int. Ed.* **2016,** *55*, 12996−13000.
(94) Gutierrez, G. D.; Coropceanu, I.; Bawendi, M. G.; Swager, T. M., A Low Reabsorbing Luminescent Solar Concentrator Employing π-Conjugated Polymers. *Adv. Mater.* **2016,** *28*, 497−501.
(95) Bouffard, J.; Swager, T. M., Fluorescent Conjugated Polymers That Incorporate Substituted 2,1,3-Benzooxadiazole and 2,1,3-Benzothiadiazole Units. *Macromolecules* **2008,** *41*, 5559−5562.

For Table of Content Only